University of Thi-Qar Journal of Science (UTJsci)
E-ISSN:2709-0256, ISSN Print: 1991-8690 Volume (10), No.1, June 2023

# Hubbard Model Calculations for Zinc Oxide Semiconductor

Aqeel Mohsin Ali
*Polymer Research Center/University of Basrah*
Basrah/ Iraq
aqeel.mohsin@uobasrah.edu.iq

***Abstract*—To investigate the effects of Hubbard on-site Coulombic correction on the structural and electronical characteristics of wurtzite zinc oxide, first-principles calculations using density functional theory (DFT) were carried out. Because of the changes in structural characteristics brought about by the correction of hybridization between Zn 3*d* and O 2*p* states, suitable Hubbard terms need to be constructed before one can make an accurate forecast of the properties of ZnO. The computations were carried out by applying Hubbard corrections U*d* to Zn 3*d* states and U*p* to O 2*p* states. These adjustments were based on the Wu-Cohen functional. When the Hubbard corrections U*d* and U*p* were introduced to the calculation, the lattice parameters were more comparable to the experimental data and were found to be accurately predicted. The combination of the correction terms U*d* and U*p* was successful in improving the underestimated bandgap of the wurtzite ZnO, which may have solved the difficulties that are associated with the traditional DFT. There is a strong agreement between the experimental bandgap and the best Hubbard parameters that were discovered for (GGA-PBE-WC+U). These parameters were found to be U*d* = 8 eV and U*p* = 8 eV.**

***Keywords*—Hubbard model, GGA-PBE-WC, ZnO, DFT, Band structure.**

## I. INTRODUCTION

Zinc oxide (ZnO) has been identified as a promising material for the development of optoelectronic and optical devices due to its large direct band gap (3.20-3.44 eV) [1]. With a binding energy of 60 meV, it finds application in a wide range of electronic gadgets, including photovoltaic cells and LEDs [2,3]. Hexagonal wurtzite-ZnO (w-ZnO) maintains a consistent crystal structure when kept at room temperature [4]. In any case, the intense pressure has caused it to take on a rock-salt structure, which may eventually lead to the compound's stabilization [5]. ZnO's electronic, optical, and structural properties have been successfully computed using density functional theory. Large structures can be modeled with great chemical accuracy using this method. For some semiconductors, the value of band gap is underestimated because the standard DFT approach accounts for the exchange-correlation functions of the GGA and LDA. w-ZnO's band gap, for example, is predicted to be 0.74 eV, which is about 70% lower than the experimental value [6-8]. Band gap problems are unfortunately common in these approaches. According to *ab initio* computation, the electronic properties of w-ZnO were calculated by Schröer and colleagues in 1993 [9]. The band gap and absolute position of 3*d* band did not match experimental results. The Zn 3*d* eigenstates exhibit highly localized and strongly correlated features. The narrow *d* bands correlation effects caused these discrepancies. Strongly correlated electronic components could not be localized due to a seemingly fatal flaw in the band gap calculation. In order to reduce the transition energy and increase the formation energy of Mott insulators, some authors have suggested using the LDA + U or the GGA + U method [10]. The original plan was to include Hubbard-type interactions U in either the LDA or the GGA to better characterize these substances. On the other hand, it has been discovered that this technique can also enhance the Hubbard parameter-based characterization of ZnO. In order to work around the limitations of traditional DFT, many researchers turn to DFT+U methods, also known as hybrid functionals. The Green's function, the B3LYP, and the Perdew-Burke-Ernzerhof (PBE) function are just a few examples [4]. Recently, Wu and Cohen (WC) proposed a new GGA exchange-energy functional [11]. Their functional, used in combination with the PBE correlation-energy functional, was shown to have significant improvement over LDA, PBE, and TPSS for the geometrical parameters and the bulk modulus of solids. However, these techniques aren't as reliable as their competitors. The low difficulty level and high computational cost of the first-principle DFT+U approach make it unsuitable for tackling the problems of complex systems. When applied to the *d* state, the Hubbard U*d* correction helps, but the ZnO bandgap is still underestimated. Recent research has shown that the U*d* and U*p* parameters, when used together, can have a positive effect on the Zn and O bandgap. In order to optimize ZnO's electronic properties and structural parameters, it is necessary to rationally tweak the values of the Hubbard parameters U*d* and U*p* [12,13]. Using the DFT+U framework, this effort seeks to identify the optimal values for the Hubbard parameters U*d*, U*p*, and GGA+U. The volume, structure, and electronic properties of ZnO determine the parameters. The Hubbard parameter values

This work is licensed under a Creative Commons Attribution 4.0 International License.
https://doi.org/10.32792/utq/utjsci/v10i1.988

obtained from DFT+U calculations with the U*d* and U*p* values were compared to those obtained from standard DFT and experimental samples.

## II. METHOD OF SIMULATION

Figure 1 shows the hexagonal ZnO crystal structure (space group 186/*P*63mc). Wurtzite ZnO has 2 zinc (Zn) and 2 oxygen (O) atoms per unit cell. Electronic, optical, and structural properties of ZnO-based materials were analyzed using first-principles calculations in Hubbard U. A comparison was made between the results and those already published. In this study, we looked at how well the CASTEP computer code performed when simulating ZnO transition oxide using the Kohn-Sham plane-wave direct Fourier transform method [14]. Wurtzite ZnO materials' electronic, optical and structural properties were analyzed using DFT from first principles. Furthermore, PBE with Wu-Cohen (PBE-WC) exchange-correlation was used to characterize the exchange-correlation [15,16]. We used a soft pseudopotential with a kinetic cutoff energy of 380 eV for this analysis. We performed the computation on a 5x5x4 k-point grid with a separation of $5x10^{-3}$ $Å^{-1}$. For the purpose of addressing the Zn *3d* electron transition, the PBE-WC+U technique was applied. Zn-$3d^{10}$ and O-$2p4$ valence electron configurations were assumed. Energy changes of less than $1 \times 10^{-5}$ eV per atom were achieved during the geometric optimization procedure. Forces up to 0.05 GPa and stresses of less than $1 \times 10^{-3}$ displaced worked well, too. In order to study the conceptual variations in the calculation, four different procedures that each made use of a unique XC functional were carried out. Initially, a conventional DFT was utilized in order to carry out the optimization procedure on the wurtzite ZnO unit cell (GGA-PBE-WC). The Hubbard term U*d* is applied to the 3*d* states of the Zn atoms by utilizing DFT+U (GGA-PBE-WC+U*d*) for the second optimization. The Hubbard term U*p* is applied to the 2*p* states of the O atoms by utilizing DFT+U (GGA-PBE-WC+U*p*) for the third optimization. The fourth optimization procedure utilized DFT+U (GGA-PBE-WC+(U*d*,U*p*)) to implement both Hubbard term U*d* to Zn 3*d* states and U*p* to O 2*p* states. The values for U*d* and U*p* ranged from 2 eV to 14 eV (step by 2) as shown at the TABLE I.

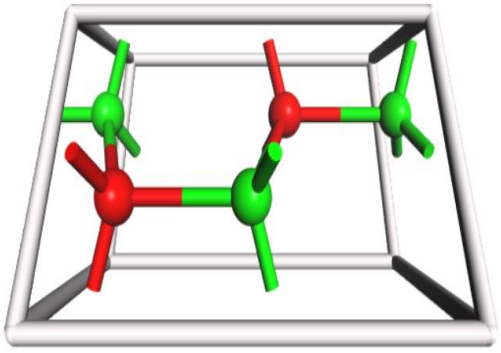

Fig. 1: Crystal structure of unit cell for wurtzite ZnO. Zn (green) and O (red).

TABLE I. Hubbard parameter values that used in the present work.

| **n** | **(Zn U*d* , O U*p*)** | | |
|---|---|---|---|
| | **(n,0)** | **(0,n)** | **(n,n)** |
| 2 | (2,0) | (0,2) | (2,2) |
| 4 | (4,0) | (0,4) | (4,4) |
| 6 | (6,0) | (0,6) | (6,6) |
| 8 | (8,0) | (0,8) | (8,8) |
| 10 | (10,0) | (0,10) | (10,10) |
| 12 | (12,0) | (0,12) | (12,12) |
| 14 | (14,0) | (0,14) | (14,14) |

## III. RESULTS

Minimizing energy and atomic forces optimized wurtzite ZnO crystal structures. The lattice parameters (*a* and *c*), lattice ratio (*c*/*a*) and volume (V) of optimized wurtzite ZnO computed from standard GGA-PBE-WC functional are compared to the experimental values listed in TABLE II. The value of lattice parameters from standard GGA-PBE-WC was consistent with each other works, which agrees with other findings [17-19]. The lattice parameters and volume from GGA-PBE-WC show a good agreement with the experimental values. On the other hand, the values of the lattice parameters GGA-PBE-WC were the same, which is in line with what other researchers have found. When compared to the other calculated lattice parameters and volume from standard GGA-PBE and GGA-PBESOL functional, the lattice parameters and volume from GGA-PBE-WC show good agreement with the experimental values, with a difference of less than 0.499%.

TABLE II: The calculated lattice parameters (*a* and *c*), lattice ratio (*c*/*a*) and volume (V) of wurtzite ZnO using standard GGA-PBE-WC with the percentage deviation (~%) from the experiment and other theoretical data ([a] - Ref. [17], [b] - Ref. [18], [c] - Ref. [19]).

| | **Exp.** | **Other works** | | **Present work** |
|---|---|---|---|---|
| | | **GGA-PBE** | **GGA-PBESOL** | **GGA-PBE-WC** |
| *a* (Å) | 3.249 [a] | 3.282 [b] (+0.98%) 3.271 [c] (+0.65%) | 3.246 [b] (–0.10%) | 3.249 (-0.028%) |
| *c* (Å) | 5.206 [a] | 5.294 [b] (+1.69%) 5.235 [c] (+0.55%) | 5.232 [b] (+0.49%) | 5.230 (+0.455%) |
| *c*/*a* | 1.602 [a] | 1.613 [b] (+0.68%) 1.600 [c] (–0.12%) | 1.611 [b] (+0.59%) | 1.610 (+0.499%) |
| V (Å$^3$) | 47.59 [a] | 49.38 [b] (+3.75%) 47.76 [c] (+0.34%) | 47.75 [b] (+0.33%) | 47.797 (+0.420%) |

In order to achieve maximum efficiency in the formation of crystals, research has been conducted on the incorporation of the U*d* and U*p* parameters into the three-dimensional states of Zn and O atoms. The GGA-PBE-WC+U functional were utilized in order to conduct an investigation into the impacts of this parameter on the volume and lattice characteristics of ZnO. By gradually increasing the Hubbard U*d* parameter, which ranged from 2 to 14 eV, it was possible to examine the changes that occurred in the range of the *a* and *c* lattice parameters. This falls in accord with the findings of other researchers who used the CASTEP software to conduct tests that were quite comparable to this one. The GGA-PBE-WC+U functional incorporation of the U*d* parameter was utilized so that the lattice parameters of ZnO could be calculated. Figure 2 show *a* lattice parameter as a function of (U*d*,0), (0,U*p*) and (U*d*,U*p*), where the value of the *a* lattice parameter is identical to the experimental value of 3.249 or 3.250 (Å) when U*d* is equal to 2, 4, 6 and 8 eV. These experimental values are shown by horizontal dashes in the graph. However, the trend lines (0,U*p*) and (U*d*,U*p*) of the lattice parameters *a* do not reach the experimental value and tend toward smaller values.

Figure 3 show *c* lattice parameter as a function of (U*d*,0), (0,U*p*) and (U*d*,U*p*), where the value of the *c* lattice parameter is identical to the experimental value of 5.204 or 5.207 (Å) when U*p* and (U*d*,U*p*) are equal to 2 eV. These experimental values are shown by horizontal dashes in the graph. However, the trend lines (U*d*,0) of the lattice parameter *c* do not reach the experimental value and tend toward larger values. As a result, the lattice parameters of wurtzite ZnO were best described from GGA-PBE-WC+U at U*d* and U*p* equal to 2 eV for calculation lattice parameters *a* and *c*. The differences in the *a* and *c* values of the ZnO lattice, both with and without the addition of the Hubbard parameter, produce results that are superior than those obtained using the conventional DFT calculations.

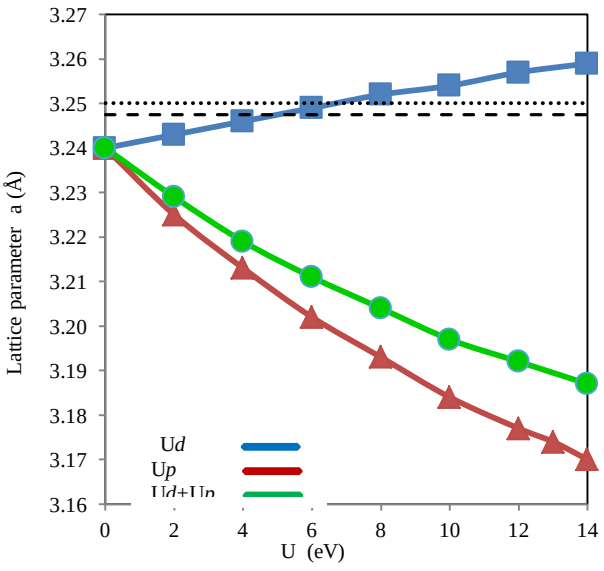


Fig. 2: Lattice parameter a of wurtzite ZnO with respect to Hubbard parameter. Horizontal dashed lines represent the experimental values.

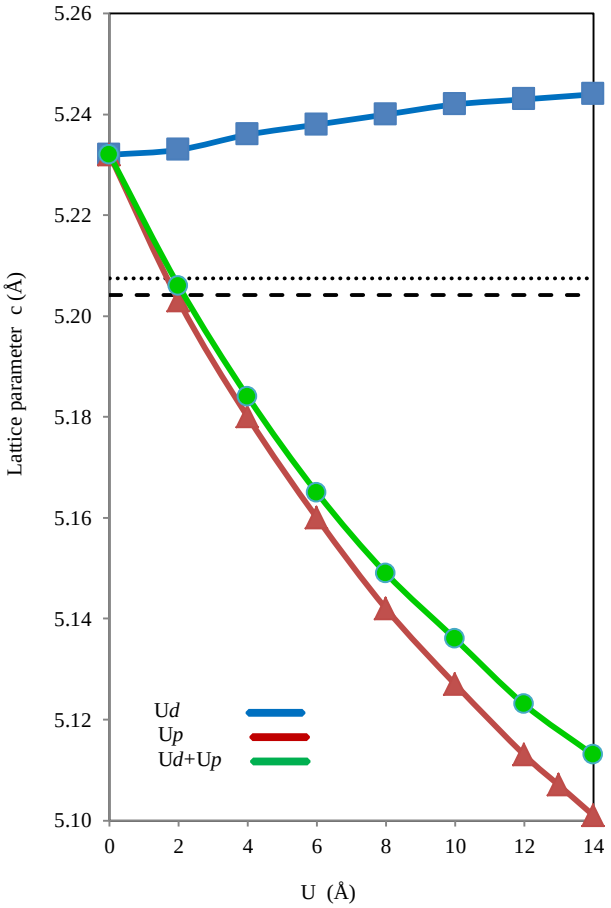


Fig. 3: Lattice parameter c of wurtzite ZnO with respect to Hubbard parameter. Horizontal dashed lines represent the experimental values.

Figure 4 illustrates the different band gap values that can be expected from wurtzite ZnO depending on whether or not the Hubbard parameter U*d* and U*p* are included and are applied to Zn and O for the functional. The values of U*d* and U*p* increased from 2 eV to 14 eV, which resulted in an increase in the band gap values. At a band gap energy of U*d* = 14 eV, the band gaps with the highest values are 1.173 eV. Even though the inclusion of the Hubbard U*d* parameter aims to correct the localized 3*d* states electrons in a correlated system but is still underestimated, these band gap values are still small in comparison to the experimental value, which is 3.37 eV. This finding is consistent with research that was conducted in the past and agrees with the findings of those studies. The pervasive underestimation of band gap has highlighted the need to incorporate the 2*p* states into the calculations. Figure 4 displayed the variation band gap values of wurtzite ZnO when the Hubbard parameter U*p* was applied to O with zero U*d* value. At a band gap energy of U*p* = 14 eV, the band gaps with the highest values are 3.361 eV, and it is very close to the experimental band gap. With equalized U*d* and U*p* values, the band gap values increased progressively as the Hubbard parameters (U*d*,U*p*) increased from 2 eV to 14 eV. To study the band gap properties of wurtzite ZnO, the appropriate values of U*d* and U*p* must be determined. Using the same CASTEP software, the selection of Hubbard U*d* value is

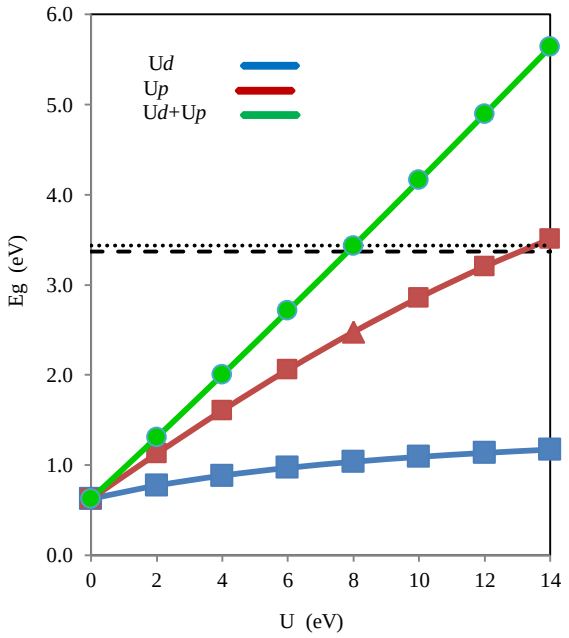


Fig. 4: Band gap of wurtzite ZnO with respect to Hubbard parameter. Horizontal dashed lines represent the experimental values

typically in the range of 8 eV, whereas the selection of U*p* is in the range of 8 eV.

Consequently, this demonstrates that the inclusion of both Hubbard parameters, U*d* and U*p*, has effectively reproduced the correct band gap of wurtzite ZnO in comparison to the standard GGA+PBE-WC. The Hubbard parameters U*d* and U*p* values for electronic properties are not the same as the values for structural properties, but the problem is to correct the underestimated band gap of wurtzite ZnO from standard DFT by including Hubbard parameter U*d* applied to the Zn-3*d* state and Hubbard parameter U*p* applied to the O-2*p* state.

Figure 5 and 6 display the band structures that were computed for wurtzite ZnO by utilizing a conventional GGA-PBE-WC functional and the best Hubbard parameters U*d* and U*p* along the highest symmetry direction of the Brillouin zone path. The band gap of wurtzite ZnO was approximately 0.618 eV when estimated using conventional GGA-PBE-WC and the result showed that it was 81% lower than the experimental values. This value is in good accord with the results of the other first-principle DFT calculations. The failure of typical GGA-PBE-WC to find the binding energy in the electrons of the 3*d* states causes an overestimation of hybridization with the anion 2*p* states, which is the root cause of these difficulties. As a result, a powerful *p-d* coupling was ultimately responsible for the narrowing of the band gap. The findings suggest that the wurtzite form of ZnO possesses a direct energy band gap between the valence band of the Γ Brillouin zone and the conduction band. The band gap is found by measuring the distance between the maximum of the valence band and the minimum of the conduction band, where the Fermi level is located at the 0 eV point on the energy scale. In spite of this, the accuracy of comparisons made between relevant crystal parameters, such as lattice parameters, were not affected in any way by the band gap finding.

It is common knowledge that the ground state DFT results showing significant Coulomb correlation and XC potential between excited-state electrons might contribute to an overestimated band gap. The underestimation of the band gap that arises from the first-principle calculations can be corrected by comparing it with the findings of the experiments using the Hubbard parameters U*d* and U*p*. In the GGA-PBE-WC+U computations, the effective Hubbard parameters U*d* and U*p* have a tendency to upper shift the minimal conduction band, which results in a wider gap between the maximum valence band and the minimum conduction band. The band gap of wurtzite ZnO determined using GGA-PBE-WC+U was around 3.432 eV respectively. When compared to the results of the other first-principle DFT+U calculations, all of the band gaps values show a high level of concordance. Therefore, the band gap calculated using GGA-PBE-WC functional was only 0.19 percent off from what was seen during the experiment.

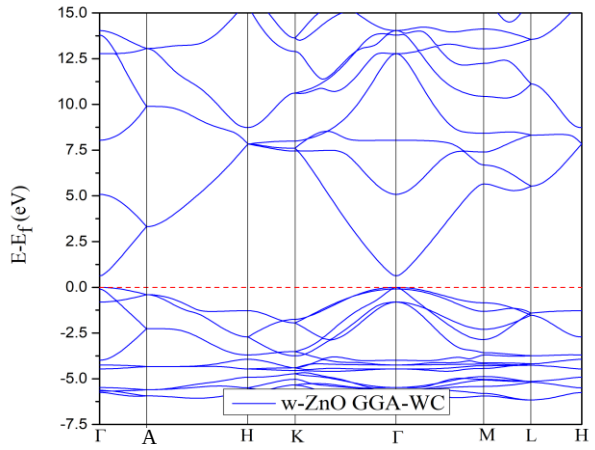


Fig. 5: The band gap structure of ZnO by using GGA-WC.

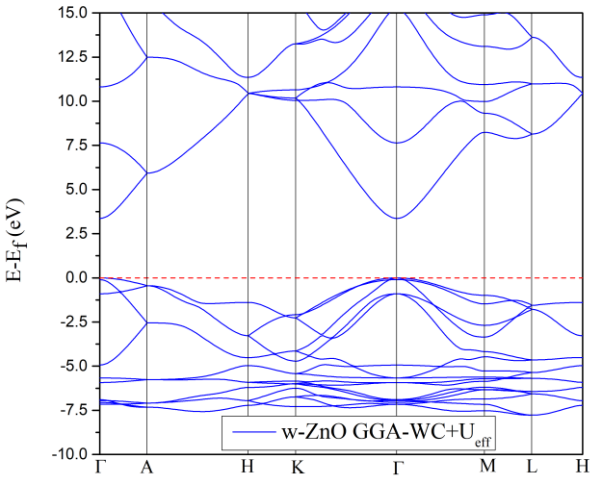


Figure 6: The band gap structure of ZnO by using GGA-WC+U*eff*. Ueff is (U*d*=8,U*p*=8).

## IV. Conclusions

First-principles calculations utilizing DFT and DFT+U methods included in CASTEP software were used in this investigation to determine the structural characteristics of wurtzite ZnO as well as its electronic properties. The incorporation of Hubbard parameters U*d* and U*p* in GGA-PBE-WC+U has highlighted a considerable difference in the structural parameters as well as the electronic structure of wurtzite ZnO. Incorporating the Hubbard parameters U*d* and U*p* has resulted in an underestimation of the wurtzite ZnO lattice parameters, but it has improved the underestimation of the band gap that was produced by traditional DFT. The properties of the computed lattice were most accurately characterized by the GGA-PBE-WC+U functional, with possible agreements of different Hubbard U*d* and U*p* values. The best Hubbard parameters of wurtzite ZnO were determined for the functional GGA-PBE-WC+U at U*d* = 8 eV and U*p* = 8 eV. These values show a high agreement with the observed band gap. According to the findings that we have obtained, the GGA-PBE-EC+U approach that was projected in order to investigate the structural and electronic properties of wurtzite ZnO appears to be an appropriate way for solving the DFT calculations problem while maintaining a low cost of computation.

## V. References


[1] N. Hamzah, M. H. Samat, N. A. Johari, A. F. A. Faizal, O. H. Hassan, A. M. M. Ali, R. Zakaria, N. H. Hussin, M. Z. A. Yahya and M. F. M. Taib "First principle LDA+U and GGA+U calculations on structural and electronic properties of wurtzite ZnO" Solid State Science and Technology, Vol. 30, No. 1 & 2, pp. 20-36, 2022.

[2] B. Mehmood, M. I. Khan, M. Iqbal, A. Mahmood and W. Al-Masry "Structural and optical properties of Ti and Cu co-doped ZnO thin films for photovoltaic applications of dye sensitized solar cells" International Journal of Energy Research. Vol. 45, No. 2, 2445, 2021.

[3] E. Cerrato, C. Gionco, M. C. Paganini and E. Giamello "Photoactivity properties of ZnO doped with cerium ions: an EPR study" Journal of Physics: Condensed Matter, Vol. 29, No. 44, 444001, 2017.

[4] K. Harun, N. A. Salleh, B. Deghfel, M. K. Yaakob and A. A. Mohamad "DFT + U calculations for electronic, structural, and optical properties of ZnO wurtzite structure: A review" Results in Physics, Vol. 16, 102829, 2020.

[5] Ü. Özgür, Y. I. Alivov, C. L. A. Teke, M. A. Reshchikov, S. Doğan, V. Avrutin, S.-J. Cho and H. Morkoç "A comprehensive review of ZnO materials and devices" JOURNAL OF APPLIED PHYSICS, Vol. 98, 041301, 2005.

[6] A. A. Mohamad, M. S. Hassan, M. K. Yaakob, M. F. M. Taib, F. W. Badrudin and O. H. Hassan "First-principles calculation on electronic properties of zinc oxide by zinc–air system" Journal of King Saud University - Engineering Science, Vol. 29, pp. 278–83, 2017.

[7] G.Y. Yao, G.H. Fann, F. Zhao, J.H. Ma, J. Chen, S.W. Zheng, S.M. Zeng, L.F He and T. Zhang "In assisted realization of p-type C-doped ZnO: a first-principles study" Physica B, Vol. 407, pp. 3539–3542, 2012.

[8] K. Harun, M. K. Yaakob, M. F. M Taib, B. Sahraoui, Z. Ahmad and A. A. Mohamad "Efficient diagnostics of the electronic and optical properties of defective ZnO nanoparticles synthesized using the sol–gel method: experimental and theoretical studies" Material Research Express, Vol. 4, 085908, 2017.

[9] P. Schröer, P. Krüger and J. Pollmann "First-principles calculation of the electronic structure of the wurtzite semiconductors ZnO and ZnS" Physical Review B, Vol. 47, 6971, 1993.

[10] V. Ivády, K. Szasz, A. L. Falk, P. V. Klimov, D. J. Christle, E. Janzén, I. Abrikosov, D. D. Awschalom and A. Gali "Theoretical model of dynamic spin polarization of nuclei coupled to paramagnetic point defects in diamond and silicon carbide" Physical Review B, Vol. 92, 115206, 2015.

[11] Z. Wu and R. E. Cohen "A More Accurate Generalized Gradient Approximation for Solids" Physical Review B, Vol. 73, 235116, 2006.

[12] Y. S. Lee, Y. C. Peng, J. H. Lu, Y. R. Zhu and H. C. Wu "Electronic and optical properties of Ga-doped ZnO" Thin Solid Films, Vol. 570, Part B, pp. 464-470, 2014.

[13] G. Shao "Red Shift in Manganese- and Iron-Doped $TiO_2$: A DFT+U Analysis" Journal of physical chemistry C, Vol. 113, No. 16, pp. 6800-6808, 2009.

[14] S. J. Clark, M. D. Segall, C. J. Pickard, P. J. Hasnip, M. I. J. Probert, K. Refson, and M. C. Payne, "First principles methods using CASTEP" Zeitschrift für kristallographie-crystalline materials, Vol. 220, No. 5-6, pp. 567-570, 2005.

[15] Z. G. Wu and R. E. Cohen "More accurate generalized gradient approximation for solids" Physical Review B, Vol. 73, 235116, 2006.

[16] Q. Liu and Z. Liu "First-principles generalized gradient approximation + U study of cubic CuAl2O4" Physical Review B, Vol. 78, 197102, 2008.

[17] S. Desgreniers "High-density phases of ZnO: Structural and compressive parameters" Physical Review B, Vol. 58, 14102, 1998.

[18] N. Hamzah, M. H. Samat, N. A. Johari, A. F. A. Faizal, O. H. Hassan, A. M. M. Ali, R. Zakaria, N. H. Hussin, M. Z. A. Yahya and M. F. M. Taib "First-Principle LDA+U and GGA+U Calculations on Structural and Electronic Properties of Wurtzite ZnO" Solid State Science and Technology, Vol. 30, No 1 & 2, pp. 20-36, 2022.

[19] M. K. Yaakob, N. H. Hussin, M. F. M. Taib, T. I. T. Kudin, O. H. Hassan, A. M. M. Ali and M. Z. A. Yahya "First Principles LDA+U Calculations for ZnO Materials" Integrated Ferroelectrics: An International Journal, Vol. 155, No. 1, pp. 15-22, 2014.